RSC Advances

ROYAL SOCIETY OF CHEMISTRY

www.rsc.org/advances

Potential of hyphenated ultra-high performance liquid chromatography-scheduled multiple reaction monitoring algorithm for large-scale quantitative analysis of traditional Chinese medicines

Qingqing Song,[a,b,#] Yuelin Song,[a,#,*] Na Zhang,[a,b] Jun Li,[a] Yong Jiang,[c] Kerong Zhang,[d] Qian Zhang,[a] and Pengfei Tu [a*]

[a] *Modern Research Center for Traditional Chinese Medicine, Beijing University of Chinese Medicine, Beijing 100029, China;*

[b] *School of Chinese Materia Medica, Beijing University of Chinese Medicine, Beijing 100102, China;*

[c] *State Key Laboratory of Natural and Biomimetic Drugs, School of Pharmaceutical Sciences, Peking University, Beijing 100191, China;*

[d] *Application Support Center, AB SCIEX, Shanghai 200233, China.*

[#] These two authors contribute equally to this article.

*Correspondence to:

Dr. Yuelin Song, E-mail: syltwc2005@163.com, Tel./fax: +86-10-6428 6100;

Prof. Pengfei Tu, E-mail: pengfeitu@163.com, Tel./fax: +86-10-8280 2750.

Abstract

It is a great challenge to perform quality control for traditional Chinese medicines (TCMs) that contain a great mount of constituents, by holistically monitoring hydrophilic and hydrophobic substances. Theoretically, the relatively low scan rate of triple quadrupole (QqQ) equipment is quite difficult to meet the demands of reliable quantitation for the narrow peaks generated from ultra-high performance liquid chromatography (UHPLC). Scheduled multiple reaction monitoring (sMRM) algorithm offers the potential to simultaneously monitor numerous analytes without compromising data quality, in particular for co-eluting compounds, by automatically altering the dwell time to maintain desired cycle time on QqQ analytical platform. In current study, UHPLC and sMRM were hyphenated to develop a practical and robust quantitative method for as many as 133 TCM-derived components, including polar and apolar compounds. Efficient separation was achieved on a coreshell-type column, Capcell core ADME column, whose functional group is adamantylethyl group to generate appropriate surface polarity along with hydrophobicity in comparison with RP-C_{18} and HILIC columns. To verify the applicability of the developed UHPLC-sMRM method, a formula was simulated by mixing eight TCM raw materials that related to those 133 analytes. Moreover, enhanced product ion scans were triggered by sMRM to generate MS^2 spectra to enhance the confidence of peak assignment. Method validation results suggested the developed method to be accurate, precise, and reproducible. In comparison with conventional MRM, sMRM was proved to be advantageous at sensitivity and precision, as well as the dependent MS^2 spectral quality. Above all, our current study indicated that the integration of UHPLC and sMRM provides the potential to globally and simultaneously quantify the components in TCMs.

Keywords: Scheduled multiple reaction monitoring; Traditional Chinese medicines; Large-scale quantitative analysis; Hybrid triple quadrupole-linear ion trap mass spectrometer; Capcell core ADME column.

1. Introduction

Traditional Chinese medicines (TCMs) have been utilized for the prevention and treatment of human diseases in China for centuries, as well as some East Asian countries.[1] Because of the long historical clinical practices and convincing therapeutic outcomes, TCMs is stimulating scientists' interests all over the world and increasing number of famous pharmaceutical companies are employing TCMs as an ideal library for the discovery of leading compounds. However, the features of TCMs include systematism, multi-target, and multi-channel efficacy attributing to their complicated chemical compositions.[2-6] If only a few ingredients are emphasized, the holistic and synergic instincts of TCMs will be neglected, and it thus calls for a comprehensive analytical approach which could reflect the quantitative characteristics of most constituents in TCMs, especially those variations relating to the pharmacological and healthy benefits, as well as toxic potential.[7] Currently, the technical obstacles to draw a complete picture for the quality of TCMs mainly lie on the characterization of hydrophilic constituents and detection of trace substances. Hydrophilic constituents have been revealed primary contributions for some famous crude drugs, *e.g.*, nucleosides and nucleobases for Cordyceps,[8, 9] and also, some amino acids are employed as the quality indicators for some raw materials, such as Pheretima and Cervi Cornu Pantotrichum. Moreover, a number of minor and trace constituents sourced from TCMs have been demonstrated attractive biological activities, *e.g.*, triterpenoid-diterpenoid heterodimers from *Pseudolarix amabilis*,[10] and a dimeric sesquiterpene lactone from *Inula japonica*.[11] Therefore, there is an urgent need to develop an analytical method featured high sensitivity and separation efficiency for globally quantitative analysis of the constituents in TCMs.

Hyphenated liquid chromatography-mass spectrometry (LC-MS) based analytical platform is currently the workhorse of quality control of TCMs. In comparison with time-of-flight (TOF) MS, multiple reaction monitoring (MRM) mode on triple quadrupole (QqQ) MS equipment exhibits superiority at linear dynamic range that

spans five to six orders of magnitude; however, QqQ-MS is disadvantageous at scan rate (0.5–4 Hz for QqQ versus 20 Hz for TOF).[12-14] Owing to the adoption of sub-2.0 μm particles, the peak width generated by ultra-high performance liquid chromatography (UHPLC) is usually much narrower than that obtained *via* conventional LC separations, generally in the region of 2–10 s width at the base, thus providing much greater peak capacity. Recently, coreshell-type particles are introduced to pack column, and they could make analytes spend less time diffusing into and out of the pores of those particles. Hence, the coreshell-type columns with approximately 3.0 μm particles could provide comparable peak capacity and width with sub-2.0 μm particles embedded column, nonetheless, offering lower back-pressure.[15] Therefore, the hyphenation of MRM with UHPLC equipped with coreshell-type column is expected as a promising tool for simultaneous determination of a dozen of components in TCMs. However, when more than one hundred constituents are desired to be concerned, acquiring sufficient data points for each narrow peak will be beyond the potency of QqQ equipment due to its slow scan rate. In general, more than ten data points are required for each peak to achieve precise determination.[16] It is feasible to synchronize the UHPLC and QqQ domain by splitting all precursor-to-product ion transitions into several separate runs and/or replacing UHPLC with HPLC to broaden the peaks; however, those two solutions are extremely contrary to the achievement of time- and labor-saving targets. Fortunately, schedule MRM (sMRM, also known as dynamic MRM) algorithm has been disclosed the potential to simultaneously monitor hundreds of metabolites by monitoring every MRM ion pair in its expected retention time window, consequently decreasing the number of concurrent ion transitions.[17-19] With the application of the sMRM algorithm, both of the cycle time and the dwell time are automatically adjusted to be appropriate, leading to the increment of data points for each chromatographic peak.[20-24] In addition, one of the most important advantages of hybrid QqQ-linear ion trap (Q-trap) equipment is that it enables to simultaneously carry out quantitative and qualitative

analyses without compromising data quality through triggering enhanced product ion (EPI) scans by certain survey experiment, such as MRM and enhanced MS scan.

In order to remove the technical barriers for large-scale quantitative analysis of TCMs, we thereby integrated the merits of UHPLC and Q-trap equipments by integrating coreshell-type column, sMRM algorithm, and EPI experiment. As many as 133 TCM-derived compounds, including both hydrophilic and hydrophobic ones, were collected to develop and validate an accurate, sensitive, and precise UHPLC-sMRM method, and a simulate TCM formula consisting of eight common raw materials, including Ginseng Radix, Aconiti Lateralis Radix Praeparata, Solani Melongenae Radix, Pheretima, Galli Gigerii Endothelium Corneum, Cistanches Herba, Polygalae Radix, and Draconis Resina, was utilized to confirm the applicability of the developed method. The findings obtained in current study are expected to propose a robust and flexible solution for the holistic quality control of TCMs.

2. Experimental

2.1 Chemicals and reagents

Seventeen amino acids, including L-alanine, L-serine, L-valine, L-threonine, L-leucine, L-isoleucine, asparagine, aspartic acid, L-phenylalanine, L-proline, L-tyrosine, L-lysine, glutamine, glutamic acid, γ-aminobutyric acid, L-histidine, L-arginine, and nine nucleosides and nucleobases, namely adenine, uracil, thymine, cytidine, guanosine, uridine, adenosine, thymidine, and inosine, were purchased from Xinjingke Biotechnology Company (Beijing, China). Sixteen ginsenosides, such as ginsenosides Rb1, Rb2, Rh1, Rh2, Rc, Rd, Re, Ro, Rf, Rg1, Rg2, Rg3, F1, F2, pseudo-ginsenoside F11, and compound K, as well as seven diterpenoid alkaloids, namely songorine, neoline, talatisamine, benzoylmesaconine, benzoylaconine, benzoylhypaconine, and hypaconitine were obtained from Shanghai Standard Biotech Co. Ltd (Shanghai, China). Several organic acids, namely citric acid, fumaric acid,

malic acid, tartaric acid, shikimic acid, malonic acid, succinic acid, quinic acid, lactic acid, adipic acid, maleic acid, ascorbic acid, nicotinic acid, and salicylic acid, were provided by Sigma-Aldrich (St Louis, MO, USA). Cinnamic acid was acquired from Sinopharm Chemical Reagent Co. Ltd (Beijing, China). Maltose and rhamnose were acquired from Shanghai Yuanye Biotech Co. Ltd (Shanghai, China). Galactitol, 3,4-dimethoxyphenylethanol, betaine, gallic acid, vanillic acid, nicotinamide, 8-*epi*-loganic acid, 3,4-dihydroxyphenylethanol, salidroside, 6-deoxycatalpol, gluroside, cistanoside E, sibiricose A_5, sibiricose A_6, mangiferin, geniposide, ferulic acid, alaschanioside A, lancerin, echinacoside, polygalaxanthone VIII, 7-*O*-methoxyl-mangiferin, polygalaxanthone IX, lariciresinol-4′-*O*-*β*-D-glucopyranoside, *N*-*trans*-*p*-coumaroyloctopamine, tenuifoliside B, verbascoside, poliumoside, *N*-*trans*-feruloyloctopamine, isocverbascoside, 4-methoxyphenylethanol, pinoresinol-*β*-D-glucopyranoside, polygalaxanthone VII, cistanoside C, 3,6′-disinapoyl sucrose, 2'-aceylpoliumoside, isocistanoside C, tenuifoliside A, 3,4,5-trimethoxycinnamic acid, tubuloside B, cistanoside D, *p*-methoxycinnamic acid, *N*-*trans*-*p*-coumaroyltyramine, polygalaxanthone IV, 3-(4-hydroxyphenyl)-*N*-[2-(4-hydroxyphenyl)-2-methoxyethyl]-acrylamide, loureiriol, *N*-trans-feruloyltyramine, liquiritigenin, 3-(4-hydroxy-3-methoxyphenyl)-*N*-[2-(4-hydroxyphenyl)-2-methoxyethyl]-acrylamide, *N*-*trans*-feruloyl-3-methoxytyramine, polygalasaponin XXVIII, 5,7,4′-trihydroxyflavanone, cannabisin D, tenuifolin, 6-hydroxy-1,2,3,7-tetramethoxyxanthone, melongenamide B, 3,4′-dihydroxy-5-methoxystilbene, 5,7-dihydroxy-4′-methoxy-8-methylflavane, 2,4′-dihydroxy-4,6-dimethoxydihydro-chalcone, 1,2,3,6,7-pentamethoxyxanthone, 1,7-dimethoxyxanthone, *N*-*trans*-feruloyltyramine dimer, cannabisin F, melongenamide D, 4-hydroxy-2,4′-dimethoxydihydrochalcone, 1,2,3,7-tetramethoxyxanthone, pterostilbene, and 4′-hydroxy-5,7-dimethoxy-8-methylflavane were provided by the chemical library of State Key Laboratory of Natural and Biomimetic Drugs, Peking University (Beijing, China). The purity of each reference compound was determined to be more than 95%

by normalization of the peak areas detected by UHPLC–DAD–IT-TOF-MS (Shimadzu, Kyoto, Japan). All of the references are also summarized in Table 1.

Formic acid, ammonium formate, dimethylsulfoxide (DMSO), methanol, and acetonitrile (ACN) were of HPLC grade and purchased from Merck (Darmstadt, Germany). Ultrapure water was prepared in-house with a Milli-Q system (Millipore, Bedford, MA, USA). The other chemicals were of analytical grade and obtained commercially from Beijing Chemical Works (Beijing, China).

2.2 Raw materials

The raw materials of Ginseng Radix (Chinese name: *Renshen*), Aconiti Lateralis Radix Praeparata (Chinese name: *Fuzi*), Solani Melongenae Radix (Chinese name: *Qiegen*), Pheretima (Chinese name: Dilong), Galli Gigerii Endothelium Corneum (Chinese name: *Ji'neijin*), Cistanches Herba (Chinese name: *Roucongrong*), Polygalae Radix (Chinese name: *Yuanzhi*), and Draconis Resina (Chinese name: *Longxuejie*), were collected from Beijing Tongrentang Co. Ltd. (Beijing, China) and a local pharmacy (Beijing, China). All crude drugs were authenticated by one of the authors (Prof. Pengfei Tu) and deposited at the Modern Research Center for Traditional Chinese Medicine, Beijing University of Chinese Medicine (Beijing, China).

2.3 Sample preparation

All raw materials were dried using a universal oven with forced convection (FD115, Tuttlingen, Germany) at 40°C for three days. Then, each crude drug was pulverized into powder using a sample mill (model YF102, RuianYongli Pharmacy Machinery Company, Zhejiang, China) and sieved through a metal drug sieve (0.25 mm, i.d.). Thereafter, simulate formula was prepared by mixing all accurately weighed raw materials (approximately 0.20 g for each) and extracted with 20-fold volumes of 50% aqueous methanol for 30 min at 25°C in an ultrasonicator (230 V, Branson model 5510, Danburry, CT, USA). Following centrifugation at 1 500 rpm for 5 min in a centrifuge (Eppendorf, Melbourne, Australia), each supernatant was

filtered through a 0.22 μm membrane. An aliquot of (50 μL) the filtrate was 20-fold diluted with 50% aqueous methanol prior to LC-MS/MS measurement. Each raw material was treated in parallel to obtain the extract sample by extracting 0.20 g raw material with 4 mL 50% aqueous methanol. Every experiment was conducted in triplicate.

Stock solutions of all reference standards were prepared individually with methanol, DMSO or water depending on compound solubility, and stored at 4ºC until use. Then, mixed standard stock solution was prepared by gathering all stock solutions. The working standard solutions were obtained by diluting the mixed standard stock solution with 50% aqueous methanol to serial desired concentration levels. On the other side, each reference solution at appropriate concentration was generated by diluting corresponding stock solution with methanol or 50% aqueous methanol for manual optimization of those compound-dependent mass spectrometric parameters.

2.4 LC-MS/MS analysis

Liquid chromatography was conducted on a Shimadzu UHPLC system (Kyoto, Japan) that comprised of two LC-20AD$_{XR}$ solvent delivery units, a SIL-20AC$_{XR}$ auto-sampler, a CTO-20AC column oven, a DGU-20A$_{3R}$ degasser, and a CBM-20A controller. Chromatographic separation was achieved on a Capcell core ADME column (2.1 mm × 150 mm, 2.7 μm, Shiseido, Tokyo, Japan) at a flow rate of 0.4 mL/min, and the column oven was maintained at 40ºC. The mobile phase was composed of 10 mmol/L aqueous ammonium formate (A) and acetonitrile containing 0.1% formic acid (B). The gradient elution was programmed as follows: 0−5 min, 0%−2% B; 5−8 min, 2%−5% B; and 8−30 min, 5%−65% B. At the end of each run, the initial composition of mobile phase (0% B) was permitted to re-equilibrate the whole system for 5 min. The auto-sampler module was maintained at 10ºC and the injection volume was set at 2.0 μL.

Mass spectrometry was achieved on an ABSciex 5500 Q-trap® mass spectrometer (ABSciex, Foster City, CA, USA) which was equipped with Turbo V™ electrospray ionization (ESI) interface and operated in sMRM mode. Both positive and negative polarities were adopted according to the results provided by manual parameter optimization. Ion optics was tuned using standard polypropylene glycol (PPG) dilution solvent. Nitrogen was used as the nebulizer (GS1), heater (GS2), curtain (CUR), and collision gas. Ion source parameters were optimized as follows: GS1, GS2, and CUR, 55, 55, and 35 psi, respectively; ionspray needle voltage, 5500 V/–4500 V; heater gas temperature, 550ºC; collisionally activated dissociation (CAD) gas, high level. Entrance potential (EP) and collision cell exit potential (CXP) levels followed those defaulted values, whereas optimized MRM ion transitions (precursor ion-to-the most abundant product ion for each analyte), declustering potential (DP), and collision energy (CE) values for the quantitative ion transitions of all reference compounds are summarized in Table 1. In addition, a accompanied ion transition which was composed with the precursor ion and the secondary abundant fragment ion, was also utilized for each compound to meet the demands for identity confirmation at the meanwhile of quantitative analysis.[25] The detection time window for each ion transition was set as 60 s (retention time ± 30 s), and the target scan time was maintained at 1.0 s. Information dependent acquisition (IDA) method was employed to trigger two EPI scans with a criterion of 200 cps. The key parameter (CE) of EPI were set as 40 eV and –40 eV for positive and negative polarities, respectively, whereas collision energy spread (CES) was set at 35 eV for either. Analyst software (version 1.6.2, ABSciex) was used for the synchronization of whole system and for data acquisition and processing.

In addition, in order to compare sMRM and conventional MRM (cMRM) in parallel, cMRM was also performed with parameters mentioned above, except that detection time window was replaced with 10 s dwell time for each ion transition.

2.5 Method validation

For method validation, quantitative terms with respect to linearity, limit of detection (LOD), lower limit of quantification (LLOQ), and recovery were assayed. Among them, LOD and LLOQ assays were performed for all 133 targets (Table 1), whereas the other assays were carried out for 23 selected analytes (Tables S1 and S2), that exhibited abundant distributions in the simulate formula, including thymine, 1,7-dimethoxyxanthone, 1,2,3,7-tetramethoxyxanthone, 1,2,3,6,7-pentamethoxyxanthone, songorine, benzoylhypaconine, benzoylaconine, L-(+)-lactic acid, nicotinic acid, inosine, salidroside, 4-hydroxy-2,4′-dimethoxydihydrochalcone, 4′-hydroxy-5,7-dimethoxy-8-methylflavane, loureiriol, 2,4′-dihydroxy-4,6-dimethoxydihydrochalcone, 6-deoxycatalpol, alaschanioside A, polygalaxanthone IX, polygalaxanthone VIII, polygalaxanthone VII, tenuifoliside B, polygalasaponin XXVIII, and ginsenoside Rb2. The performance of each validation assay followed the protocols described in the literature.[25] For recovery assay, 23 analytes were added into mixed raw materials at low, medium, and high concentration levels before extraction to prepare desired samples (Table S2, Supplemental information B). Six replicates of the stimulate formula solution were used to evaluate the repeatability, and the sample was maintained in the auto-sampler at 15°C and then analyzed over three consecutive days to carry out stability assay. RSD% (relative standard deviation %) value of the peak area of each analyte was adopted to express the repeatability and stability.

Afterwards, the developed method was applied for the analysis of simulate formula and all raw materials.

3. Results and discussion

3.1 Development of LC-MS/MS method

3.1.1 Optimization of mass parameters

Aiming to obtain optimal quantitative response, the MS/MS fragmentation for each compound was investigated. All 133 analyte solutions were diluted to desired

concentrations (50–100 ng/mL) and directly infused into the ESI interface using a syringe pump (flow rate: 7 μL/min). Afterwards, optimization of the mass parameters, including precursor-to-product ion transitions, DP, and CE for each analyte, was manually carried out following the procedures described in the literature.[26, 27]

The mass spectrometric behaviors of ginsenosides, flavonoids, phenylpropanoid amides, phenylethanoid glycosides, xanthones, and aconite alkaloids, including pseudo-molecular ions and fragments, agreed well with some previous descriptions,[25, 28-31] while the MS patterns of those hydrophilic components were consistent with the information archived in the literature [32-35] and some accessible databases (e.g. MassBank, METLIN, and HMDB). On the other side, the mass cracking rules of those authentic references from Polygalae Radix, including sibiricose A5, sibiricose A6, mangiferin, polygalaxanthone VIII, 7-*O*-methoxylmangiferin, polygalaxanthone IX, polygalaxanthone VII, polygalaxanthone VII, polygalasaponin XXVIII, tenuifolin, 1,7-dimethoxyxanthone, 1,2,3,7-tetramethoxyxanthone and 1,2,3,6,7-pentamethoxy -xanthone, were identical with the properties documented in Ref.[36] More compounds, 98 ones in total (corresponding to 196 ion transitions), could afford better responses under negative polarity, while 35 components (corresponding to 70 ion transitions) obtained greater responses with positive ionization mode. All information regarding MS^1, MS^2, DP, CE, and quantitative MRM transitions is summarized in Table 1.

3.1.2 Selection of columns

As noted above, we simultaneously targeted both hydrophilic and hydrophobic components in current study; thus, it is of great importance to select an optimum column that could retain and separate extensive analytes across great polarity span. In general, a single column is only advantageous at retaining and separating components in a relatively narrow polarity range. However, a few new types of particles, such as pentafluorophenyl (PFP or F5) substituted particles,[24, 37] have been developed and proved for universal retention.

Several columns were introduced as candidates to pick the optimal one for comprehensive retention. After careful comparison in terms of peak capacity, retention performance, peak shape, and low back-pressure, one of the coreshell-type columns, the Capcell core ADME column, was found to be superior to the other columns, not only the versatile Phenomenex Synergi Polar-RP column[38] and the widely recommended PFP and F5 columns, but also some HILIC candidates. Some additives, such as formic acid and ammonium formate, were fortified into the mobile phase to assess whether they could advance the peak shapes along with overall MRM response, and the results suggested the addition of 10 mM ammonium formate and 0.1% formic acid into phases A and B, respectively, as an ideal choice.

The function group substituted to the silica gel of ADME particles is adamantylethyl group. Its surface polarity is 0.65,[39] which is quite higher than that of common RP-C_{18} columns (approximately 0.4) and makes those particles could retain the hydrophilic components like HILIC column. Meanwhile, the hydrophobicity of 1.98 indicates that the ADME column could exhibit comparable retention potency for hydrophobic compound with normal C_{18} column; however, it could tolerate 100% aqueous mobile phase for a long period without stationary phase collapse due to the relatively low hydrophobicity level but big size for adamantylethyl substitutions. Hence, it is not astonishing to note that coreshell-type ADME column was advantageous at peak capacity, peak shape, and back-pressure over the other columns for the retention and separation of both polar and non-polar components.

The optimized conditions for LC and MS domains were applied for the analysis of mixed references and the simulate TCM formula, and the representative chromatograms are elucidated in Fig. 1, while the corresponding chromatogram of each raw material is showed in Fig. S1 (Supplemental information A). Overall, satisfactory peak shape and separation capacity, however, low back-pressure, were gained. As shown in those chromatograms, most of the hydrophilic components gathered among 0.2–2.0 min, whereas those hydrophobic constituents widely

distributed between 2.0 and 28.0 min. Owing to the adoption of sMRM algorithm, mutual interferences between co-eluting analytes could be significantly reduced. The signals in mixed references were subjected to match with those existed in formula for signal assignment in terms of retention times, MS^2 spectra, and ion transitions, and all 133 analytes could be found in the simulate formula.

3.2 Method validation

All 133 compounds were subjected for LLOQ and LOD assays, and the results are presented at Table 1. Except for a couple of analytes, such as fumaric acid, rhamnose, 8-*epi*-loganic acid, cistanoside E, mangiferin, and compound K, LLOQs and LODs of all analytes are lower than 50 ng/mL, suggesting that sensitively quantitative analysis could be achieved using the developed UHPLC-sMRM method. It is worthwhile to mention that those toxic constituents from Aconiti Lateralis Radix Praeparata, including songorine, neoline, talatisamine, benzoylmesaconine, benzoylaconine, benzoylhypaconine, and hypaconitine, could be detected even at extremely trace concentrations.

A total of 23 analytes that were observed as the primary ingredients in the simulate formula were employed for linearity, intra- and inter-day, repeatability, stability, and recovery assays. A weight of $1/x$ was applied for the regression of calibration curves if necessary. All calibration formulae and linear ranges are elucidated in Table S1 (Supplemental information B). As described in Table S1, correlation coefficients (r) of all calibration curves were higher than 0.999 over their corresponding linear concentration ranges. All RSDs% for repeatability and stability ranged from 0.83% and 12.78%, indicating satisfactory performance in terms of repeatability and stability. Three concentration levels of the mixture of 23 analytes were utilized to assess the intra- and inter-day precisions of the developed method, and all RSD values were observed lower than 15% (Table S2, Supplemental information B), indicating that the method could meet the demands for precise determination. Moreover, known amounts (low, medium and high concentration

levels) of mixed 23 standard solutions were added to the mixed raw material powder prior to ultrasonic-assistant extraction (Table S2, Supplemental information B). The recoveries were observed between 73.96% and 139.95% for all selected analytes, while most of the related RSDs were calculated lower than 15% (Table S2, Supplemental information B).

Because tandem mass spectrometric detection acted as the additional orthogonal separation dimension and sMRM algorithm ulteriorly advanced the simultaneous determination, the mutual interferences among the co-eluting substances were expected to be mild. The responses of some selected hydrophilic analytes when they existed in mixture were almost equivalent to the corresponding response yielded by injecting single compound individually, suggesting that those interferences were negligible during the quantitative characterization. In addition, the impacts from carryover and re-injection were also assessed and the results suggested influences from them could be ignored due to their mild influences.

Above all, the developed UHPLC-sMRM method was demonstrated as a sensitive, precise, and accurate approach for simultaneous determination of numerous targets. Afterwards, the developed method was subjected for the simultaneous determination of those primary 23 components in the extraction solution of the simulate formula, and the quantitative results are elucidated in Table S1 (Supplemental information B).

3.3 Comparison of sMRM and cMRM

MRM with fixed dwell time for each ion transition has been widely proved as a promising tool for the simultaneous determination of a dozen of compounds; however, acceptable results are difficult to gain when numerous analytes are targeted. Therefore, in the highly multiplexed detection of TCMs, it is essential to employ sMRM algorithm where the mass spectrometer is scheduled to detect only a limited number of ion transitions in predefined retention time windows.[40] Significant retention time shift would result in the loss of analyte when it was only programmed to be detected in a narrow retention time window. In the present study, the retention times of all

analytes were assessed using the inter-day assays, and only minor migrations (less than 0.1 min) were observed for the retention times of those components. In consideration that most of the peak widths were approximately 10.0 s, the detection window was thereby fixed at 1.0 min for all analytes, while the target scan time was maintained at 1.0 s to satisfy the monitoring of several hydrophilic components that focused at the head of the chromatogram.

The principles of cMRM and sMRM algorithms are briefly elucidated in Fig. 2, as well as their respective representative chromatograms. In the case of cMRM, all ion transitions are always monitored in every acquisition cycle. In general, it is necessary to assign at least 10 ms dwell time to each ion pair without seriously compromising the reproducibility of the integrated peak. The cycle time was equal to the total dwell times of all ion transitions plus all pause times (Fig. 2A). In the present study, as many as 196 ion pairs were monitored under negative polarity, and the cycle time was thereby calculated as 2.1 s. For a typical UHPLC peak, the peak width was approximately 10 s; therefore, it is not astonishing that only five points were acquired for a signal peak using cMRM (Fig. 2B). On the other side, the narrow detection window (1.0 min) of sMRM reduced the number of concurrent ion transitions compared with cMRM, and the dwell time was significantly and automatically maximized without the requirement of a long cycle time (Fig. 2C). The data points of the representative signal corresponding to sMRM were more fifteen, which can meet the demands for reliable quantitation (Fig. 2D). In addition, the intensity of the peak yielded by sMRM is significant greater than that of cMRM (Fig. 2). At the meanwhile, because adequate dwell time was applied for each ion pair, the noise level of the equipment is thus obviously lower than that of cMRM (Fig. 2).

The quantitative performances of sMRM and cMRM were also elucidated. Overall, all 133 compounds were detected in the simulated formula by sMRM algorithm, whereas more than 50 analytes could not be observed with cMRM method. Twelve analytes were picked to compare the sensitivity and precision between sMRM

and cMRM. As shown in Table 2, all LODs and LLOQs resulted from sMRM are significantly lower, 5-fold at least, than those of cMRM. In particular, those hydrophilic components that gathered at the head of the chromatogram, *e.g.*, γ-aminobutyric acid, nicotinamide, thymine, adenosine, and malonic acid, could be detected at trace concentration with sMRM, whereas comparable sensitivity could not afford by cMRM (Table 2). In addition, corresponding that more data points were distributed in sMRM peak in comparison with cMRM, the RSDs% of intra-day assays of sMRM (1.44%–7.25%) were quite lower those resulted from cMRM (3.37%–24.37%).

The cycle time is of great importance not only to obtain sufficient data points for a narrow peak, but to avoid the loss of peaks when several analytes are co-eluted.[16] In the present study, EPI scans were triggered by the sMRM experiment with an IDA mode; hence, the loss of signals would result in the absence of MS^2 spectra. In addition, as aforementioned, the response of cMRM is usually significantly lower than that of sMRM, and it is thereby difficult to acquire MS^2 spectra for those minor and trace compounds, because the intensity of cMRM ion transitions might not exceed the IDA threshold. Moreover, even though the intensity of cMRM ion transition is a bit higher than the threshold, the quality of MS^2 spectra should be rough. Taken adenosine for instance, since insufficient precursor ion (*m/z* 268 $[M+H]^+$) were transmitted into linear ion trap cell (Q3), the intensity of both protonated and fragment ions in the MS^2 spectrum generated by cMRM (lower in Fig. 3) were quite lower than those in the MS^2 spectrum generated by sMRM (upper in Fig. 3). Moreover, some noise signals, such as ion species at *m/z* 251, 195, 156, and 109, are observed in the MS^2 spectra of cMRM (lower in Fig. 3), indicating a remarkable obstacle for the confirmation of the peak identity.[41]

Therefore, sMRM was regarded to be superior to cMRM at sensitive, reproducible, and reliable quantitation by providing higher responses, more data points, and high quality MS^2 spectra.

4. Conclusions

An algorithm namely sMRM was utilized to circumvent the contradiction between low scan rate of QqQ equipment and the narrow width of the peaks generated from UHPLC, and adequate data points were gained for each peak, although as many as 133 analytes, including hydrophilic and hydrophobic substances, were concerned in the current study. Efficient separation was obtained using a Capcell core ADME column. Satisfactory quality of MS^2 spectra was also achieved for all targets using EPI scans on Q-trap analytical platform attributing to the introduction of sMRM. Method validation assays indicated the developed UHPLC-sMRM method to be sensitive, accurate, and precise. Collectively, UHPLC-sMRM was suggested as a promising tool to meet the demands for large-scale quantitative analysis of both hydrophilic and hydrophobic compounds in TCMs, which could dramatically advance the quality control of TCMs in comparison with that only several hydrophobic components were concerned. In addition, we can make a prospective view that the developed system provides a feasible analytical platform to simultaneously and universally monitor polar endogenous substances and TCM-derived apolar ingredients following the treatment of TCMs.

Acknowledgements

This work was financially supported by National Science Fund of China (No. 81403073, to Y.-L.S.), the TCM support project from the Ministry of Industry and Information Technology of China (to J.L.), the Program for New Century Excellent Talents in University (No. NCET-13-0693, to J.L.), and National Science Fund for Excellent Young Scholars (No. 81222051, to Y. J.).

References

1. Y. Jiang, B. David, P. Tu and Y. Barbin, *Anal. Chim. Acta*, 2010, **657**, 9–18.

2. E. Giovannucci, D. M. Harlan, M. C. Archer, R. M. Bergenstal, S. M. Gapstur, L. A. Habel, M. Pollak, J. G. Regensteiner and D. Yee, *CA Cancer J. Clin.*, 2010, **60**, 207-221.
3. M. M. Gottesman, *Annu. Rev. Med*, 2002, **53**, 615-627.
4. J. J. Monsuez, J. C. Charniot, N. Vignat and J. Y. Artigou, *Int. J. Cardiol.*, 2010, **144**, 3-15.
5. M. E. Franks, G. R. Macpherson, E. R. Lepper, W. D. Figg and A. Sparreboom, *Drug Resist Updat*, 2003, **6**, 301-312.
6. T. Xue and R. Roy, *Science*, 2003, **300**, 740-741.
7. P. S. Xie and A. Y. Leung, *J. Chromatogr. A*, 2009, **1216**, 1933–1940.
8. P. Chen, W. Li, Q. Li, Y. Wang, Z. Li, Y. Ni and K. Koike, *Talanta*, 2011, **85**, 1634–1641.
9. P. X. Chen, S. Wang, S. Nie and M. Marcone, *J. Funct Foods*, 2013, **5**, 550–569.
10. B. Li, D. Y. Kong, Y. H. Shen, H. Yuan, R. C. Yue, Y. R. He, L. Lu, L. Shan, H. L. Li, J. Ye, X. W. Yang, J. Su, R. H. Liu and W. D. Zhang, *Org. Lett.*, 2012, **14**, 5432-5435.
11. J. J. Qin, L. Y. Wang, J. X. Zhu, H. Z. Jin, J. J. Fu, X. F. Liu, H. L. Li, W. D. Zhang, *Chem. Commun.*, 2011, **47**, 1222-1224.
12. T. Rousu, J. Herttuainen and A. Tolonen, *Rapid Commun. Mass Spectrom.*, 2010, **24**, 939-957.
13. U. Vrhovsek, D. Masuero, M. Gasperotti, P. Franceschi, L. Caputi, R. Viola and F. Mattivi, *J. Agric. Food Chem.*, 2012, **60**, 8831-8840.
14. T. Hyotylainen and S. Wiedmer, *Chromatographic Methods in Metabolomics*, The Royal Society of Chemistry, 2013, p. 44.
15. Y. L. Song, W. H. Jing, G. Du, F. Q. Yang, R. Yan and Y. T. Wang, *J. Chromatogr. A*, 2014, **1338**, 24-37.
16. T. Hyotylainen and S. Wiedmer, *Chromatographic Methods in Metabolomics*, The Royal Society of Chemistry, 2013, p. 47.
17. J. Liang, W. Y. Wu, G. X. Sun, D. D. Wang, J. J. Hou, W. Z. Yang, B. H. Jiang, X. Liu and D. A. Guo, *J. Chromatogr. A*, 2013, **1294**, 58-69.
18. J. Li, C. X. Hu, X. J. Zhao, W. D. Dai, S. L. Chen, X. Lu and G. W. Xu, *J. Chromatogr. A*, 2013, **1320**, 103-110.
19. Y. L. Song, N. Zhang, S. P. Shi, J. Li, Y. F. Zhao, Q. Zhang, Y. Jiang, and P. F. Tu, *J. Chromatogr. A*, 2015, DOI: 10.1016/j.chroma.2015.06.007, in press.
20. Y. Liu, C. E. Uboh, L. R. Soma, X. Li, F. Guan, Y. You and J. W. Chen, *Anal. Chem.*, 2011, **83**, 6834-6841.
21. J. Wang, W. Chow and W. Cheung, *J. Agric. Food Chem.*, 2011, **59**, 8589-8608.
22. M. Dziadosz, J. P. Weller, M. Klintschar and J. Teske, *J. Chromatogr. B*, 2013, **929**, 84-89.
23. F. Song, *J. Agric. Food Chem.*, 2011, **59**, 4361-4364.
24. S. Dresen, N, Ferreirós, H, Gnann, R. Zimmermann and W. Weinmann, *Anal. Bioanal. Chem.*, 2010, **396**, 2425-2434.

25. Y. L. Song, N. Zhang, Y. Jiang, J. Li, Y. F. Zhao, S. P. Shi and P. F. Tu, *RSC Adv.*, 2015, **5**, 6419-6428.
26. Y. L. Song, W. H. Jing, G. Du, F. Q. Yang, R. Yan and Y. T. Wang, *J. Chromatogr. A*, 2014, **1338**, 24-37.
27. Y. Song, W. Jing, F. Yang, Z. Shi, M. Yao, R. Yan and Y. Wang, *J. Pharm. Biomed. Anal.*, 2014, **88**, 269-277.
28. X. Q. Su, Y. L. Song, J. Zhang, H. X. Huo, Z. Huang, J. Zheng, Q. Zhang, Y. F. Zhao, W. Xiao, J. Li and P. F. Tu, *Fitoterapia*, 2014, **99**, 64-71.
29. J. Sun, Y. L. Song, J. Zhang, Z. Huang, H. X. Huo, J. Zheng, Q. Zhang, Y. F. Zhao, J. Li and P. F. Tu, *J. Agric. Food Chem.*, 2015, **63**, 3426-3436.
30. Y. Jiang, S. P. Li, Y. T. Wang, X. J. Chen and P. F. Tu, *J. Chromatogr. A*, 2009, **1216**, 2156-2162.
31. W. Z. Yang, M. Ye, X. Qiao, Q. Wang, T. Bo and D. A. Guo, *Eur. J. Mass Spectrom.*, 2012, **18**, 493-503.
32. J. Qu, W. Chen, G. Luo, Y. Wang, S. Xiao, Z. Ling and G. Chen, *Analyst*, 2002, **127**, 66-69.
33. P. Purwaha, P. L. Lorenzi, L. P. Silva, D. H. Hawke and J. N. Weinstein, *Metabolomics*, 2014, **10**, 909-919.
34. C. Stentoft, M. Vestergaard, P. Lovendahl, N. B. Kristensen, J. M. Moorby and S. K. Jensen, *J. Chromatogr. A*, 2014, **1356**, 197-210.
35. D. Bylund, S. H. Norstrom, S. A. Essen and U. S. Lundstrom, *J. Chromatogr. A*, 2007, **1176**, 89-93.
36. Y. Ling, Z. Li, M. Chen, Z. Sun, M. Fan and C. Huang, *J. Pharm. Biomed. Anal.*, 2013, **85**, 1-13.
37. H. Yoshida, T. Mizukoshi, K. Hirayama and H. Miyano., *J. Agric. Food Chem.*, 2007, **55**, 551-560.
38. T. J. Whelan, M. J. Gray, P. J. Slonecker, R. A. Shalliker and M. A. Wilson, *J. Chromatogr. A*, 2005, **1097**, 148-156.
39. T. Mochizuki, T. Takayama, K. Todoroki, K. Inoue, J. Z. Min and T. Toyo'oka, *Anal. Chim. Acta*, 2015, **875**, 73-82.
40. L. Guo, Y. Xiao and Y. Wang, *Anal. Chem.*, 2014, **86**, 10700-10707.
41. Z. Yan, T. Li, P. Lv, X. Li, C. Zhou and X. Yang, *J. Chromatogr. B*, 2013, **928**, 22-31.

544 **Figure legends**

545 **Fig. 1** Overlaid extracted ion current (EIC) chromatograms.

546 (A) EIC chromatograms of all 70 ion transitions monitored under positive polarity for
547 mixed references; (B) EIC chromatograms of all 70 ion transitions monitored under
548 positive polarity for the simulate TCM formula; (C) EIC chromatograms of all 196
549 ion transitions monitored under negative polarity for mixed references; (D) EIC
550 chromatograms of all 196 ion transitions monitored under negative polarity for the
551 simulate TCM formula.

552 **Fig. 2** Comparisons of algorithm principles and chromatograms acquired in parallel
553 using cMRM and sMRM.

554 (A) Overlaid EIC chromatograms of all 196 ion transitions monitored under negative
555 polarity for mixed references using cMRM algorithm. All ion transitions are always
556 monitored in every acquisition cycle, and the cycle time is equal to the total dwell
557 times of all ion transitions plus all pause times. (B) Representative peak acquired
558 using cMRM. Because the cycle time is too long for the peak width, the data points of
559 this signal are only five, which cannot meet the demands for reliable quantitation. (C)
560 Overlaid EIC chromatograms of all 196 ion transitions monitored under negative
561 polarity for mixed references using sMRM algorithm. Each ion transition is only
562 monitored in its expected retention time window. In the current case, MRM detection
563 window for each ion transition is fixed as 1.0 min, whereas both of the cycle time and
564 the dwell time are automatically adjusted to be appropriate. (D) Representative peak
565 acquired using sMRM. Because the cycle time is automatically adjusted, and usually
566 less than the target scan time (1.0 s), the data points of this signal are more fifteen,
567 which can meet the demands for reliable quantitation.

568 **Fig. 3** Representative MS^2 spectra (adenosine) were acquired by enhanced product ion
569 experiments which were triggered by sMRM (upper) and cMRM (lower). Obviously,
570 the intensity of most fragments of sMRM is higher than those of cMRM, and also,
571 some noise signals are observed in the MS^2 spectra of cMRM.

Table 1 Retention times (t_R), MS^1 and MS^2 spectral information, compound-dependent mass parameters, limits of detection (LODs) and lower limits of quantification (LLOQs) for 133 analytes.

No.	Compound	t_R (min)	MS^1 (*m/z*)	MS^2 (*m/z*) [a]	DP (V)	CE (eV)	LOD (pg/mL)	LLOQ (pg/mL)
1	Citric acid	0.74	191	129;**111**;87;85	-30	-13	128	8.00×10^3
2	Fumaric acid	0.75	115	**71**	-35	-15	1.60×10^4	2.00×10^5
3	D-Malic acid	0.75	133	**115**;89;71;43	-40	-20	5.12	8.00×10^3
4	D-Tartaric acid	0.75	149	103;**87**;73	-20	-16	128	8.00×10^3
5	(-)-Shikimic acid	0.75	173	155;137;129;**111**;93;73	-70	-15	4.00×10^4	2.00×10^5
6	Glutamic acid	0.76	148	**84**	25	23	2.56	12.8
7	Aspartic acid	0.77	134	**74**	25	21	8.00×10^3	4.00×10^4
8	L-Proline	0.78	116	**70**	50	20	1.02	12.8
9	Glutamine	0.79	147	130;**84**	25	25	1.02	25.60
10	Malonic acid	0.79	103	**59**	-40	-15	8.00×10^3	1.60×10^4
11	Succinic acid	0.79	117	99;**73**	-35	-12	8.00×10^3	1.60×10^4
12	Quinic acid	0.79	191	**173**;127;85	-100	-23	3.20×10^3	1.60×10^4
13	L-Serine	0.80	106	**60**	40	16	1.02	2.56
14	Asparagine	0.82	133	**74**	30	23	128	640
15	L-(+)-Lactic acid	0.82	89	**43**	-40	-14	128	2.00×10^5
16	L-Threonine	0.84	120	**102**	30	10	12.80	1.60×10^3
17	L-Alanine	0.85	90	**44**	25	17	8.00×10^3	1.60×10^4
18	γ-Aminobutyric acid	0.85	104	**87**	40	16	1.02	2.56
19	Galactitol	0.86	181	**163**;113;101;85;71	-100	-16	6.40×10^3	8.00×10^4
20	3,4-Dimethoxyphenylethanol	0.86	181	**89**	-40	-16	1.16×10^4	7.28×10^5
21	Betaine	0.89	118	**58**	40	41	0.51	5.12
22	L-Arginine	0.90	175	157;130;116;**70**	25	32	667	1.67×10^4

23	Adipic acid	0.90	145	127;**101**;83	-35	-21	1.60×10^{3}	1.60×10^{4}
24	Gallic acid	0.90	169	151;**125**;97;81	-60	-21	1.28×10^{3}	3.20×10^{3}
25	L-Histidine	0.91	156	128;**110**	25	21	1.02	5.12
26	Maleic acid	0.96	115	**71**	-35	-15	64	128
27	Maltose	0.96	341	179;143;113;**89**;71	-80	-30	51.20	640
28	Rhamnose	0.97	163	**73**	-35	-20	2.00×10^{6}	4.00×10^{6}
29	L-Valine	0.98	118	**72**	25	18	1.02	12.80
30	L-Ascorbic acid	1.25	175	**115**;87;71;59	-40	-14	64	128
31	Uracil	1.54	113	**96**	40	27	4.00×10^{4}	1.00×10^{5}
32	L-Isoleucine	1.63	132	115;**86**	50	18	3.20×10^{3}	1.60×10^{4}
33	L-Tyrosine	1.63	182	165;147;**136**;123	25	19	1.60×10^{3}	8.00×10^{3}
34	Nicotinic acid	1.76	122	94;**78**	-50	-20	8.00×10^{3}	1.60×10^{4}
35	L-Leucine	1.81	132	114;**86**	50	18	3.20×10^{3}	1.60×10^{4}
36	Cytidine	2.11	244	128;**112**	25	17	1.28×10^{3}	3.20×10^{3}
37	Uridine	2.65	245	227;**113**;107	40	23	3.20×10^{3}	1.60×10^{4}
38	Vanillic acid	3.22	167	152;**123**;108	-50	-16	1.60×10^{4}	8.00×10^{4}
39	Thymine	3.92	127	**110**	40	23	1.28×10^{3}	6.40×10^{3}
40	Inosine	4.88	267	**135**;92	-80	-30	3.20×10^{3}	6.40×10^{3}
41	L-Phenylalanine	5.00	166	**120**;103	50	19	3.20×10^{3}	8.00×10^{3}
42	Guanosine	5.51	284	**152**;135;110	40	25	1.28×10^{3}	6.40×10^{3}
43	Nicotinamide	6.16	123	107;**80**	30	30	5.12	1.28×10^{3}
44	Adenine	6.51	134	**107**;92;65	-70	-18	6.40×10^{2}	3.20×10^{3}
45	Salicylic acid	6.77	137	**93**;65	-50	-21	1.60×10^{3}	8.00×10^{3}
46	8-*epi*-Loganic acid	7.62	375	**213**;169;151	-130	-22	4.00×10^{5}	4.00×10^{6}
47	Thymidine	8.20	243	225;131;**127**	30	16	6.40×10^{3}	1.60×10^{4}
48	3,4-Dihydroxyphenylethanol	8.29	153	**123**;105;93;77	-40	-20	4.93×10^{3}	4.93×10^{4}

49	Adenosine	9.29	268	**136**;119	40	30	1.28×10^{3}	6.40×10^{3}
50	Salidroside	11.40	299	**119**;89	-130	-20	3.20×10^{3}	1.60×10^{4}
51	6-Deoxycatalpol	11.47	345	299;**165**;101	-50	-12	1.60×10^{4}	3.20×10^{4}
52	Gluroside	12.31	331	**161**;125;107	-30	-15	3.20×10^{4}	1.60×10^{5}
53	Cistanoside E	12.50	475	329;**161**;134	-30	-53	2.00×10^{6}	4.00×10^{6}
54	Sibiricose A_5	12.94	517	**175**;160	-190	-32	1.02	25.60
55	Sibiricose A_6	13.27	547	529;**205**;190	-200	-31	1.02	12.80
56	Songorine	13.40	358	**340**;165;153;115	100	39	< 0.10	< 0.10
57	Mangiferin	13.56	421	403;385;**331**;301	-140	-31	4.00×10^{4}	2.00×10^{6}
58	Geniposide	13.62	387	355;**225**;123;101	-100	-12	3.20×10^{3}	6.40×10^{3}
59	Ferulic acid	13.89	193	178;149;**134**;117;106	-60	-21	256	1.28×10^{3}
60	Alaschanioside A	14.01	537	375;357;**327**;312;136	-80	-35	640	6.40×10^{3}
61	Lancerin	14.33	405	369;**285**;169	-160	-33	1.02	25.60
62	Neoline	14.57	438	**420**;356;221;152;122	120	40	< 0.10	< 0.10
63	Echinacoside	14.83	785	623;477;461;**161**;133	-30	-53	3.20×10^{3}	1.60×10^{4}
64	Polygalaxanthone VIII	15.17	567	447;**345**;315	-130	-42	320	640
65	7-*O*-Methoxyl-mangiferin	15.27	435	417;345;**315**	-140	-30	25.60	320
66	Talatisamine	15.30	422	**390**;358;181;169;129	120	39	< 0.10	< 0.10
67	Polygalaxanthone IX	15.84	551	505;431;**243**;201	-130	-36	25.60	320
68	Lariciresinol-4′-*O*-*β*-D-glucopyranoside	15.88	521	359;**329**;192;121	-60	-30	51.20	640
69	*N*-*trans*-*p*-Coumaroyloctopamine	15.98	298	**280**;145;133;119	-160	-17	191.36	956.80
70	Tenuifoliside B	16.10	667	461;**205**;190	-200	-37	25.60	320
71	Verbascoside	16.17	623	461;315;**161**;133	-50	-41	3.20×10^{3}	6.40×10^{3}
72	Poliumoside	16.21	769	607;461;**161**;133	-50	-55	3.20×10^{3}	1.60×10^{4}
73	*N*-*trans*-Feruloyloctopamine	16.48	328	**310**;161;133	-120	-18	1.68	42.11
74	Isoverbascoside	16.58	623	461;315;**161**;133	-50	-41	3.20×10^{3}	6.40×10^{3}

75	4-Methoxyphenylethanol	16.65	151	**136**;108;92;59	-40	-17	3.11	7.78
76	Pinoresinol-*β*-D-glucopyranoside	16.70	519	**357**;342;151;136	-60	-24	51.20	1.28×10^3
77	Polygalaxanthone VII	16.76	611	596;576;368;**303**	-130	-42	320	640
78	Cistanoside C	17.26	637	491;475;**161**;133	-50	-44	1.28×10^3	6.40×10^3
79	3,6'-Disinapoyl sucrose	17.29	753	547;367;325;**205**;190	-200	-39	0.51	1.02
80	2′-Aceylpoliumoside	17.49	811	769;649;607;**161**;133	-50	-54	3.20×10^3	6.40×10^3
81	Isocistanoside C	17.63	637	491;473;461;**161**;133	-50	-44	1.60×10^4	6.40×10^3
82	Cinnamic acid	17.83	147	**103**;62	-50	-15	8.00×10^3	1.60×10^4
83	Tenuifoliside A	18.01	681	**443**;179;137	-200	-34	0.20	1.02
84	3,4,5-Trimethoxycinnamic acid	18.13	237	178;**133**;103;89	-50	-17	6.40×10^3	3.20×10^4
85	Tubuloside B	18.22	665	623;461;443;315;**161**;133	-50	-45	6.40×10^3	1.60×10^4
86	Benzoylmesaconine	18.24	590	572;**540**;166;105	90	48	< 0.10	< 0.10
87	Ginsenoside Rg1	18.36	845	**799**;637;475;437;391	-90	-32	2.00×10^4	4.00×10^4
88	Ginsenoside Re	18.38	991	**945**;637	-90	-32	6.00×10^3	8.00×10^3
89	Cistanoside D	18.47	651	615;505;193;**175**;160	-50	-37	51.20	640
90	*p*-Methoxycinnamic acid	18.55	177	149;**133**;118;107	-50	-15	1.60×10^4	3.20×10^4
91	*N-trans-p*-Coumaroyltyramine	18.66	282	145;**119**;117	-120	-34	1.45	7.24
92	Polygalaxanthone IV	18.70	565	521;344;**257**;242;172	-200	-40	8.00×10^3	8.00×10^4
93	3-(4-Hydroxyphenyl)-*N*-[2-(4-hydroxyphenyl)-2-methoxyethyl]-acrylamide	18.81	312	**280**;145;117	-50	-17	4.01	20.03
94	Loureiriol	19.06	301	**195**;167;123	-90	-24	2.06	3.10
95	*N-trans*-Feruloyltyramine	19.07	312	297;178;**148**;135	-130	-36	40.06	200.32
96	Liquiritigenin	19.14	255	**135**;119;91	-100	-23	1.05	5.24
97	3-(4-Hydroxy-3-methoxyphenyl)-*N*-[2-(4-hydroxyphenyl)-2-methoxyethyl] acrylamide	19.23	342	324;**310**;160;133	-95	-17	43.90	219.52
98	*N-trans*-Feruloyl-3-methoxytyramine	19.44	342	327;298;**148**;135	-120	-35	4.39	43.90

99	Polygalasaponin XXVIII	19.68	1103	**1103;**745;583;539;469; 455;425;	-70	-20	3.20×10^{3}	4.00×10^{3}
100	Benzoylaconine	19.70	604	572;**554**;522;199;105	100	47	< 0.10	< 0.10
101	Benzoylhypacoitine	20.23	574	**542**;510;178;105	103	47	< 0.10	< 0.10
102	Pseudo-ginsenoside F11	20.63	845	**799**;653;491	-90	-32	4.00×10^{3}	2.00×10^{4}
103	5,7,4′-Trihydroxyflavanone	20.70	271	177;**151**;119;93;65	-100	-25	5.58	139.55
104	Ginsenoside Rf	20.71	845	**799**;637;475;459;391	-90	-32	4.00×10^{3}	2.00×10^{4}
105	Cannabisin D	20.80	623	**460**;444;350;322;310;158	-190	-38	1.60	3.19
106	Ginsenoside Ro	20.80	955	**955**;793;569;523	-90	-5	8.00×10^{3}	4.00×10^{4}
107	Tenuifolin	21.20	679	625;**455**;425;342	-70	-38	128	320
108	6-Hydroxy-1,2,3,7-tetramethoxyxanthone	21.22	331	316;**301**;157;89	-180	-28	128	320
109	Melongenamide B	21.41	639	621;486;460;415;**297**	-40	-44	81.92	1.02×10^{3}
110	Ginsenoside Rb1	21.53	1153	**1107**;945;799;783	-90	-32	1.00×10^{5}	2.50×10^{6}
111	Ginsenoside Rg2	21.66	829	**783**;637;475;391	-90	-32	2.00×10^{4}	4.00×10^{4}
112	Ginsenoside Rc	21.91	1123	**1077**;945;915;783;621;459	-90	-32	8.00×10^{3}	1.00×10^{4}
113	3,4′-Dihydroxy-5-methoxystilbene	22.05	241	**225**;197;181;143	-145	-29	123.55	1.54×10^{3}
114	5,7-Dihydroxy-4′-methoxy-8-methylflavane	22.08	285	191;165;**119**;79	-130	-28	9.16×10^{3}	4.58×10^{4}
115	Ginsenoside Rh1	22.14	683	**637**;475;391	-90	-32	4.00×10^{3}	8.00×10^{3}
116	Ginsenoside Rb2	22.18	1123	**1077**;945;915;783;621;459	-90	-32	4.00×10^{3}	8.00×10^{3}
117	2,4′-Dihydroxy-4,6-dimethoxydihydrochalcone	22.63	301	**207**;147;135;93	-40	-24	6.19	154.85
118	Ginsenoside Rd	22.87	991	**945**;917;783;621;459	-90	-32	2.00×10^{4}	4.00×10^{4}
119	Hypaconitine	23.08	616	584;**556**;524;496;338;197	130	44	< 0.10	< 0.10
120	Ginsenoside F1	23.11	683	**637**;475;391;71	-90	-32	4.00×10^{3}	8.00×10^{3}
121	1,2,3,6,7-Pentamethoxyxanthone	23.21	347	**332**;317;289;218;121	100	27	1.02	5.12

122	1,7-Dimethoxyxanthone	23.40	257	**242**;213;171;139;115	120	30	2.56	5.12
123	*N-trans*-Feruloyltyramine dimer	23.43	623	**460**;445;430;324;297	-200	-30	1.60	7.99
124	Cannabisin F	23.56	623	471;**432**;402;298	-30	-39	3.19	39.94
125	Melongenamide D	23.93	934	**771**;739;580;395;319	-100	-50	119.68	598.40
126	4-Hydroxy-2,4′-dimethoxydihydrochalcone	24.43	285	181;**149**;134;117	-80	-19	1.83×10^3	1.83×10^4
127	1,2,3,7-Tetramethoxyxanthone	24.82	317	**287**;259;215;186;132	130	35	1.02	5.12
128	Ginsenoside F2	25.68	829	**783**;621;459;375;99	-90	-32	2.00×10^4	4.00×10^4
129	Ginsenoside Rg3	25.91	829	**783**;621;459	-90	-32	2.00×10^4	4.00×10^4
130	Pterostilbene	25.92	255	**239**;224;197;169	-100	-30	5.23	26.17
131	4′-Hydroxy-5,7-dimethoxy-8-methylflavane	27.96	299	179;**119**	-20	-18	9.60×10^3	4.80×10^4
132	Ginsenoside Rh2	29.63	667	**621**;581;459;417	-90	-32	4.00×10^3	6.00×10^3
133	Compound K	30.16	667	**621**;459;339;161	-90	-32	2.00×10^5	5.00×10^5

[a] Product ions in bold are selected for quantitative analysis.

Table 2 Comparison of the chromatographic performance between sMRM and conventional MRM (cMRM) algorithms in terms of sensitivity and precision.

Compound	sMRM			cMRM		
	LOD (ng/mL)	LLOQ (ng/mL)	Intra-day RSD (%) [a]	LOD (ng/mL)	LLOQ (ng/mL)	Intra-day RSD (%)
γ-Aminobutyric acid	0.0010	0.0026	7.25	0.13	1.60	14.12
Nicotinamide	0.0051	0.010	2.62	6.40	16.0	3.37
Thymine	1.28	6.40	4.19	6.40	16.0	14.78
Adenosine	1.28	6.40	5.84	16.00	32.0	7.25
Malonic acid	8.00	16.0	3.59	200.00	400.0	9.21
Cinnamic acid	8.00	16.0	2.66	40.00	200.0	6.13
3,4-Dihydroxyphenylethanol	4.93	49.3	3.31	24.60	123.2	24.37
Inosine	3.20	6.40	4.90	16.00	200.0	10.35
Salidroside	3.20	16.0	2.93	44.00	200.0	7.14
Polygalaxanthone IV	8.00	80.0	4.27	40.00	200.0	5.37
Echinacoside	3.20	16.0	1.44	16.00	80.0	6.83
Ginsenoside Rf	4.00	20.0	3.27	20.00	100.0	13.45

[a] Precision data was evaluated by the relative standard deviations (RSDs) of intra-day (n = 6).

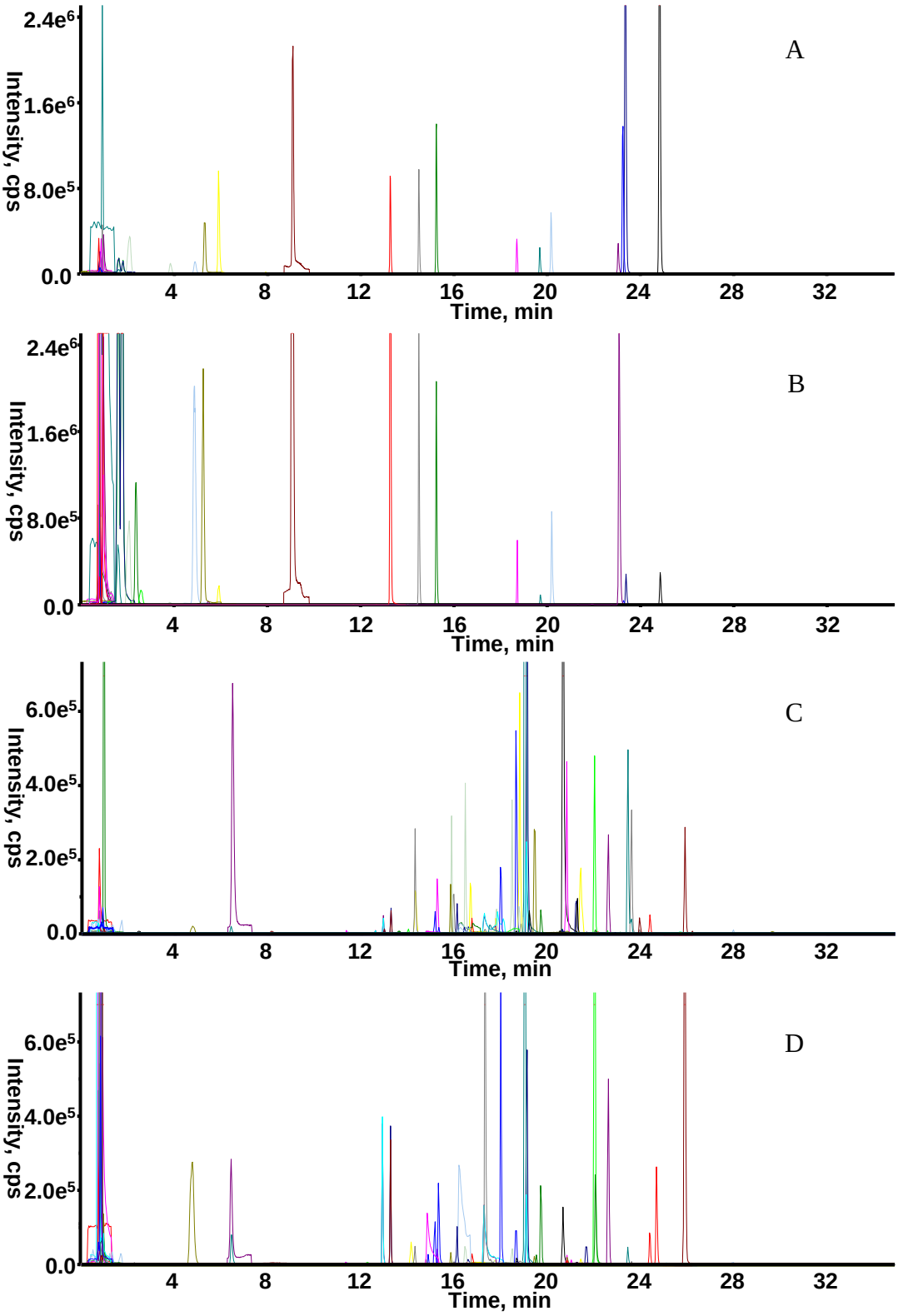

Fig. 1

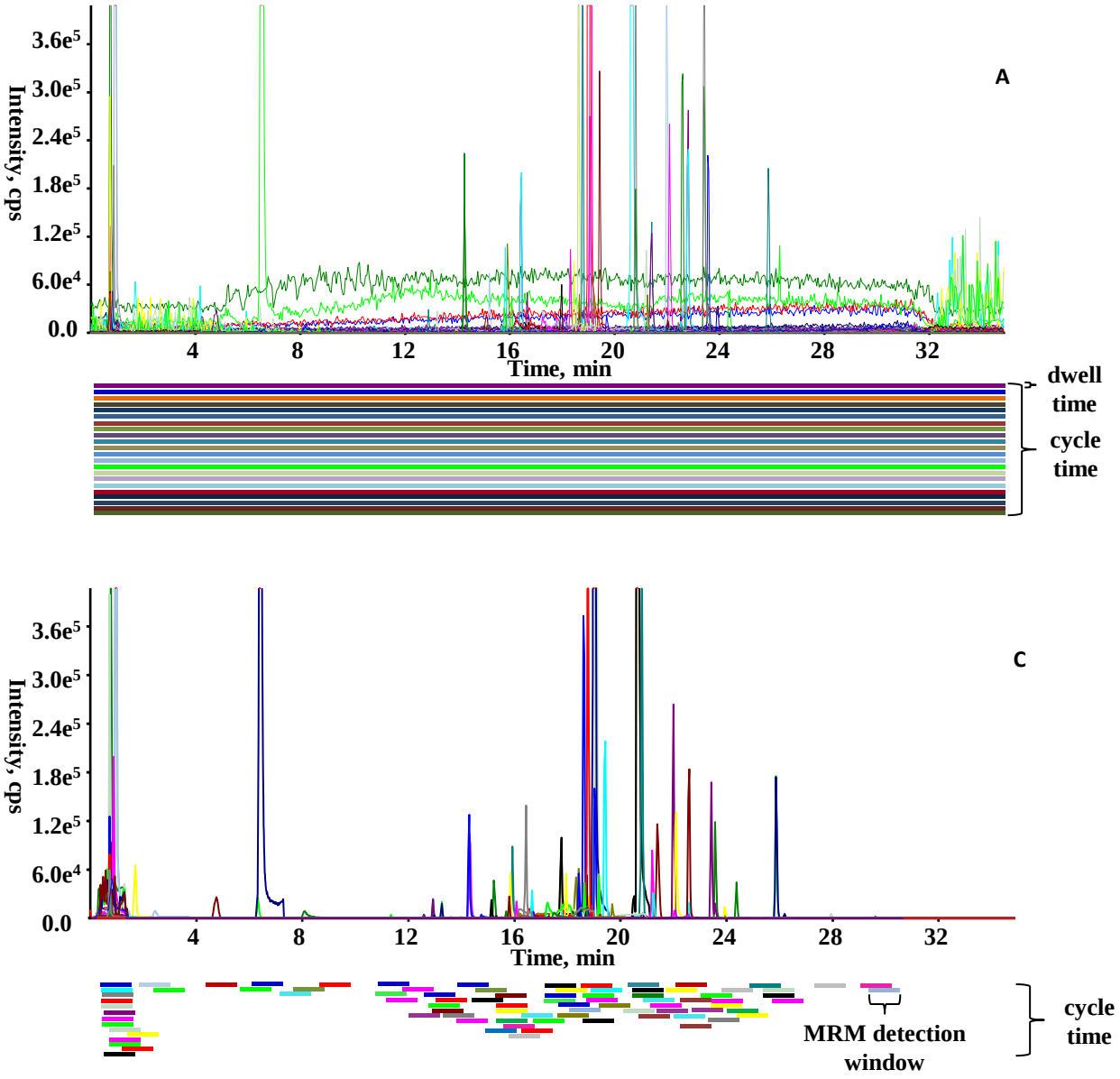

Fig. 2

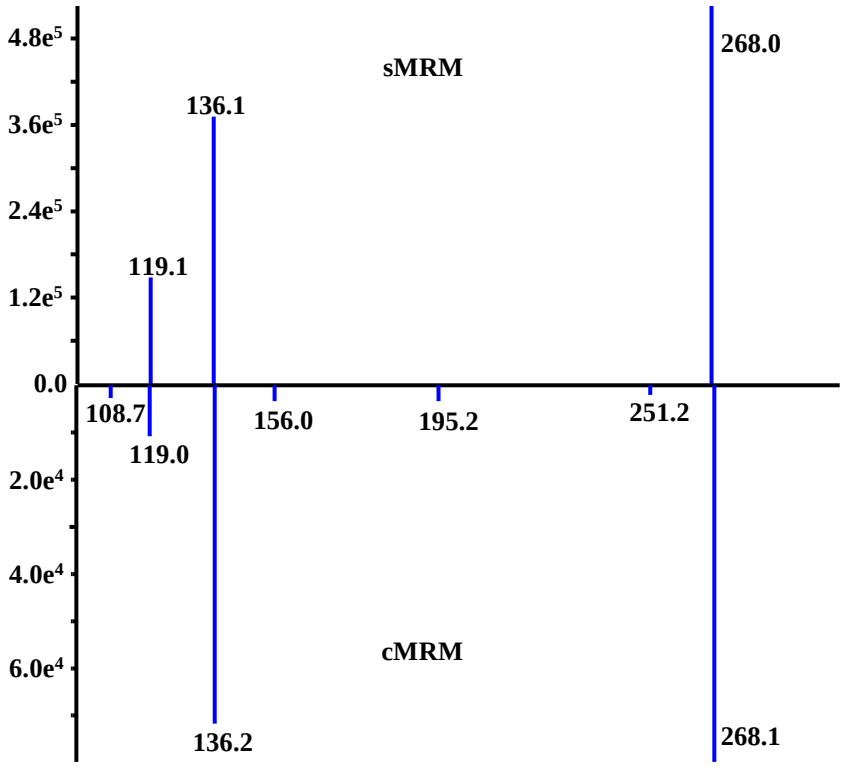

Fig. 3